

# A Backup System for Automotive Steer-by-Wire, Actuated by Selective Braking

Alejandro D. Dominguez-Garcia  
Laboratory for Electromagnetic  
and Electronic Systems  
Massachusetts Institute of Technology  
Cambridge, MA 02139-4307  
USA  
Email: aledan@MIT.EDU

John G. Kassakian  
Laboratory for Electromagnetic  
and Electronic Systems  
Massachusetts Institute of Technology  
Cambridge, MA 02139-4307  
USA  
Email: jgk@MIT.EDU

Joel E. Schindall  
Laboratory for Electromagnetic  
and Electronic Systems  
Massachusetts Institute of Technology  
Cambridge, MA 02139-4307  
USA  
Email: joels@MIT.EDU

**Abstract**—In this paper we propose an alternate approach to improve Steer-by-Wire (SbW) reliability in which we utilize Brake-Actuated Steering (BAS) as an independent secondary backup steering system. In SbW systems, component and module redundancy is the common approach used to maintain the steering function when a failure occurs. Unfortunately this adds a significant amount of complexity and cost and, what is more important, it is not possible to overcome unanticipated and common mode failures of the SbW system. BAS utilizes the torque generated by selective wheel braking and/or acceleration to actuate the steering mechanism. With this approach, if the primary steering system (SbW) fails uncovered or there is a common mode failure, the steering rack is decoupled from the primary steering actuator and the wheels are instead steered by the torque generated by application of asymmetric braking (or acceleration). BAS, as well as SbW, will be a heavy user of power electronics, electrical actuators, sensors and sophisticated control systems, many of which are already available from electronic stability systems (e.g., ESP), which are becoming more common in passenger cars. In this paper we detail the characteristics of the BAS system and provide the models necessary for designing appropriate power electronics and control systems.

## I. INTRODUCTION

Safety critical systems in a car, for example, hydraulic brakes and power steering, require a secondary or backup activation mechanism to prevent catastrophic failure. These backup mechanisms should be based ultimately upon differentiated redundant systems to avoid unanticipated and common mode failures of the main system.

In a conventional power assisted steering system, the mechanical connection between the driver and the steering rack serves as the secondary steering mechanism [1]. In a SbW system the secondary steering mechanism cannot rely on a mechanical link (e.g., the steering column) between the steering wheel and the steering rack since the goal of SbW is to eliminate such a mechanical connection. Lacking this connection, SbW design efforts have focused on developing fault-tolerant systems based on redundancy, i.e., the duplication of components and modules at all levels [1], [2], [3], [4]. This solution is widely applied in aircraft, but it adds a significant amount of complexity and cost and, what is more important, it is not possible to overcome unanticipated and common mode

failures. Therefore, it is important to explore alternatives to classical redundancy for achieving system integrity. In this paper we propose an independent backup steering system, Brake-Actuated Steering (BAS), based on utilizing already-existing systems to implement selective wheel braking and/or acceleration to actuate the steering mechanism. Similar approaches have been proposed by NASA, in order to develop the technology for future aircraft designs for emergency flight control, using engine thrust to augment or replace the flight control system [5].

BAS, as well as SbW, will use power electronics, electrical actuators, sensors and sophisticated control systems, some of which are already available from electronic stability systems, (e.g., ESP), which are becoming more common in passenger cars. Here, we detail the characteristics of the BAS system and provide the models necessary for designing appropriate power electronic and control systems.

Section II of this paper explains the underlying motivation for developing this new system. Section III presents the dynamic model of the system used in the simulations. In Section IV, the control strategy is presented. Section V shows some simulation results, comparing the behavior of a model implementing BAS to that of a vehicle with a conventional steering system. Concluding remarks and future work are presented in Section VI. The notation used is listed at the end of the paper.

## II. SELECTIVE BRAKING AS A BACKUP STEERING SYSTEM FOR STEER-BY-WIRE

Selective braking is already used in ABS as a means of controlling the vehicle in the presence of skidding conditions, and in electronic stability systems, which keep the vehicle from exercising maneuvers that could result in loss of control, e.g., rollovers [6]. In stability systems, selective braking is used as a means of maintaining the yaw rate and the body slip angle of the vehicle below the limits that could result in the loss of controllability and stability. However, such systems do not take complete control of the steering task, they only help stabilize the car in an oversteer or understeer situation.

A promising way to utilize already-existing systems to meet the need for a secondary mechanism to maintain steering capability, when an uncovered failure or a common cause failure occurs in the SbW system, is to directly control the road wheel angle, (and thus, also the body slip angle and the yaw rate), by utilizing the selective braking capability already incorporated in vehicles equipped with electronic stability systems. In the unlikely event that SbW fails, the steering actuator is disconnected and the driver command (as indicated by the steering wheel angle) is used to generate selective braking (accelerating) forces on each wheel [7]. The moments produced at each wheel by the offset (at road level) between the longitudinal center plane of the wheel and the kingpin axis (the scrub radius) cause the front wheels to turn appropriately. It appears that such a system, with appropriate control, could exhibit dynamic behavior similar to that of the primary steering mechanism (SbW). This contrasts sharply with conventional mechanical backup systems, which require a large torque at the steering wheel if the power assist suddenly fails while turning. In such a situation an unprepared driver may lose control of the car.

### III. SYSTEM MODEL

In this section, we present the model used in the development of the control strategy. First, a two-track vehicle dynamics model is developed. This model has been augmented so that the differential longitudinal forces at the front and rear tires  $\Delta F_{lf}$ ,  $\Delta F_{lr}$ , as well as the road wheel angle  $\delta$ , are available as inputs. A simplified model for the road wheel actuator is then presented, in which the driver command no longer produces any effect in the steering rack. Finally, the road wheel actuator model is coupled with the vehicle dynamics model to obtain the complete system model in which the control inputs are only the differential longitudinal force at front and rear tires  $\Delta F_{lf}$ ,  $\Delta F_{lr}$ . This simplified model allows us to run fast simulations using *Matlab/Simulink*, giving us good insight to the performance of BAS.

#### A. Vehicle dynamics model

The vehicle dynamics model presented here is developed in a manner similar to the development of the linear single-track model [8]. We extend the linear single-track model to a linear two-track model by also considering the differential longitudinal forces acting at the front and rear tires as control inputs, and making the following assumptions:

- No lateral load transfer
- No longitudinal load transfer
- No rolling or pitching motions (on the body)
- The tire slip angles are small enough to consider the tire working in the linear part of the tire-slip angle characteristic (i.e., the lateral forces acting on the tires are proportional to the slip angle)
- Constant forward velocity
- No aerodynamic effects
- A small-angle approximation is made for the road wheel angle  $\delta$

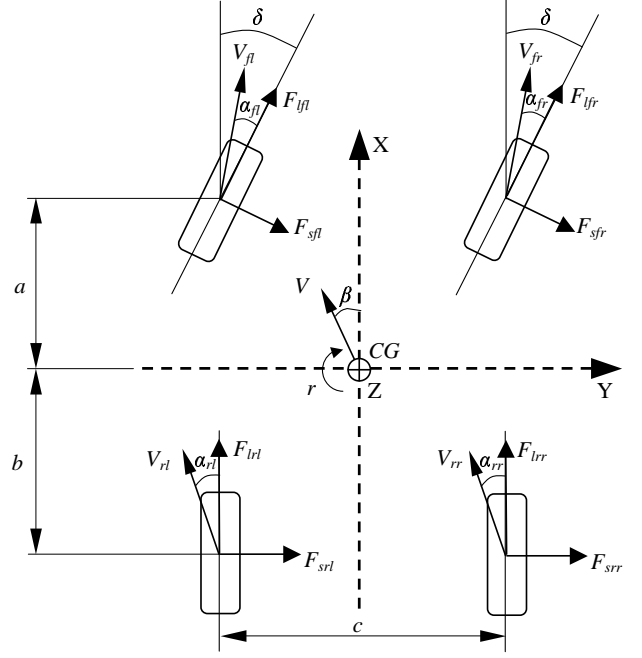


Fig. 1. Vehicle variables and parameters for the linear two-track model.

Figure 1 defines the geometric parameters used in the state-space representation of the vehicle dynamics model given by (1). As defined in the figure, all vehicle variables and parameters are positive, except for the body slip angle  $\beta$ , and the tire slip angles  $\alpha_{fl}$ ,  $\alpha_{fr}$ ,  $\alpha_{rl}$ ,  $\alpha_{rr}$ , which are defined as negative. The influences of the road wheel angle  $\delta$  (which is no longer controlled directly by the driver), and the differential longitudinal forces at the front and rear tires  $\Delta F_{lf}$ ,  $\Delta F_{lr}$ , have been separated. The longitudinal tire forces are the new variables controlled by the driver via the steering wheel angle  $\delta_w$ . Equation (1) represents the lateral motion and the rotation around the center of gravity (CG). Equation (2) represents the longitudinal motion of the vehicle (there is no longitudinal acceleration term since constant forward velocity is assumed). The lateral forces acting on the tires are assumed to be equal at the right and left tires of the same axle. They are represented by equations (3) and (4).

$$\begin{bmatrix} \dot{\beta} \\ \dot{r} \end{bmatrix} = \begin{bmatrix} \frac{C_f + C_r}{mV} & \frac{aC_f - bC_r}{mV^2} - 1 \\ \frac{aC_f - bC_r}{J} & \frac{a^2C_f + b^2C_r}{VJ} \end{bmatrix} \begin{bmatrix} \beta \\ r \end{bmatrix} + \begin{bmatrix} \frac{-C_f}{mV} \\ \frac{-aC_f}{J} \end{bmatrix} \delta + \begin{bmatrix} 0 & 0 \\ \frac{c}{2} & -\frac{c}{2} \end{bmatrix} \begin{bmatrix} \Delta F_{lf} \\ \Delta F_{lr} \end{bmatrix} \quad (1)$$

$$F_{lfl} + F_{lfr} + F_{lrl} + F_{lrr} = 0 \quad (2)$$

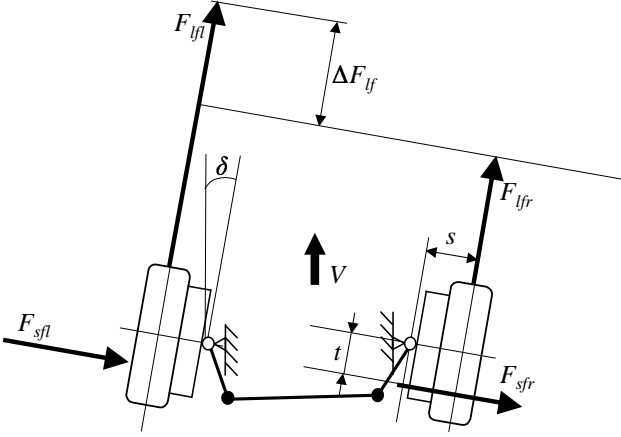


Fig. 2. Top view of a simplified road wheel actuator.

$$F_{sfl} = F_{sfr} = \frac{C_f}{2} \left( \beta + \frac{ar}{V} - \delta \right) \quad (3)$$

$$F_{srl} = F_{srr} = \frac{C_f}{2} \left( \beta - \frac{br}{V} \right) \quad (4)$$

### B. Road wheel actuator model

The assumptions made to develop the road wheel actuator model are summarized as follows:

- The kingpin axis is vertical, and kingpin inertia and friction are neglected
- Tire forces are the only mechanisms to generate torque around the kingpin axis, i.e., there is no force transmitted from the steering rack
- Effect of suspension, steering rack and column compliances are neglected

Figure 2 shows a top view of a simplified road wheel actuator geometry, defining the parameters involved in the road wheel actuator model given by (5). As defined in the figure, all variables and parameters are positive, including the scrub radius  $s$ , displayed also as positive for simplicity of the picture, although it is negative in most commercial cars. The road wheel angle  $\delta$  depends on the vehicle states  $\beta$  and  $r$  and also on the differential longitudinal force at the front tires  $\Delta F_{lf}$ .

$$\delta = \beta + \frac{a}{v}r - \frac{s}{C_f t} \Delta F_{lf} \quad (5)$$

### C. Coupled road wheel actuator and vehicle dynamics model

By substituting (5) into (1), the complete vehicle model (6) is obtained. The limitation on the longitudinal forces imposed by (2) remains the same.

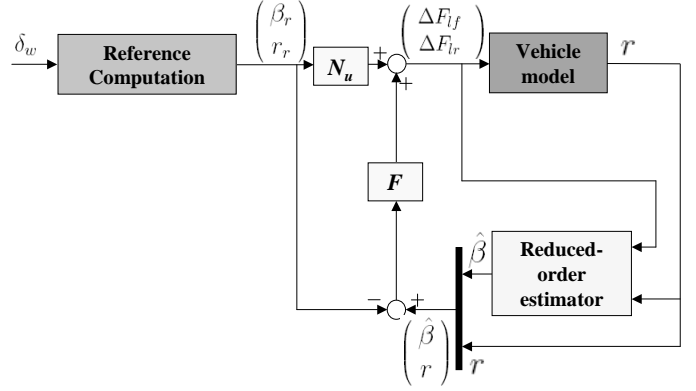


Fig. 3. Closed-loop control system block diagram.

$$\begin{bmatrix} \dot{\beta} \\ \dot{r} \end{bmatrix} = \begin{bmatrix} \frac{C_r}{m \cdot V} & \frac{-bC_r}{mV^2} - 1 \\ \frac{-bC_r}{J} & \frac{b^2 C_r}{VJ} \end{bmatrix} \begin{bmatrix} \beta \\ r \end{bmatrix} + \begin{bmatrix} \frac{s}{tm \cdot V} & 0 \\ \frac{c}{2} + \frac{as}{tJ} & \frac{c}{2} \end{bmatrix} \begin{bmatrix} \Delta F_{lf} \\ \Delta F_{lr} \end{bmatrix} \quad (6)$$

## IV. CONTROL SYSTEM

Figure 3 defines the structure of the control system. The input reference for the system is computed using a linear single-track vehicle dynamics model [8], which is a simplified model of the dynamic behavior of a vehicle with a conventional steering system. The input reference is introduced to the system in such a way that the tracking error is zero. The feedback control law is designed using the pole-placement technique, which will yield a similar transient behavior to that of the linear single-track model. A reduced-order estimator is used to estimate the value of the body slip angle, since the only measurement available for the control system is the yaw rate. This is due to the fact that in electronic stability systems, the body slip angle is estimated rather than being directly measured.

### A. Reference computation

Equation (7) represents the linear single-track model. It defines the dynamics of a vehicle with a conventional steering system, in which the steering compliance was neglected.

$$\begin{bmatrix} \dot{\beta}_r \\ \dot{r}_r \end{bmatrix} = \begin{bmatrix} \frac{C_f + C_r}{mV} & \frac{aC_f - bC_r}{mV^2} - 1 \\ \frac{a \cdot C_f - bC_r}{J} & \frac{a^2 C_f + b^2 C_r}{VJ} \end{bmatrix} \begin{bmatrix} \beta_r \\ r_r \end{bmatrix} + \begin{bmatrix} \frac{-C_f}{mV} \\ \frac{-aC_f}{J} \end{bmatrix} \frac{\delta_w}{SR} \quad (7)$$

By setting  $\dot{\beta}$  and  $\dot{r}$  to zero, a relation between  $\delta_w$  and the vehicle states  $\beta_r$  and  $r_r$  is obtained (8), which is the input reference to the system.

$$\begin{bmatrix} \beta_r \\ r_r \end{bmatrix} = - \begin{bmatrix} \frac{C_f + C_r}{mV} & \frac{aC_f - bC_r}{mV^2} - 1 \\ \frac{aC_f - bC_r}{J} & \frac{a^2C_f + b^2C_r}{VJ} \end{bmatrix}^{-1} \times \begin{bmatrix} \frac{-C_f}{mV} \\ \frac{-aC_f}{J} \end{bmatrix} \frac{\delta_w}{SR} \quad (8)$$

Equation (9) yields the appropriate value of the matrix  $N_u$  that makes the system track the reference input.

$$N_u = - \begin{bmatrix} \frac{s}{tmV} & 0 \\ \frac{c}{2} + \frac{as}{tJ} & \frac{c}{2} \end{bmatrix}^{-1} \begin{bmatrix} \frac{C_r}{mV} & \frac{-bC_r}{mV^2} - 1 \\ \frac{-bC_r}{J} & \frac{b^2C_r}{VJ} \end{bmatrix} \quad (9)$$

### B. Feedback control law

Equation (10) gives the structure of the feedback control law [9], where  $N_u$  is the zero steady-state error matrix gain and  $F$  is the state feedback matrix.

$$\begin{bmatrix} \Delta F_{lf} \\ \Delta F_{lr} \end{bmatrix} = F \begin{bmatrix} \beta \\ r \end{bmatrix} + (N_u - F) \begin{bmatrix} \beta_r \\ r_r \end{bmatrix} \quad (10)$$

The pole placement technique is used to compute the value of the State feedback matrix  $F$ , matching the poles of the closed-loop system with those corresponding to the linear single-track model. The structure of the matrix  $F$  is such that only the differential longitudinal force at the front tires  $\Delta F_{lf}$  is affected. The structure of the matrix  $F$  is given by (11).

$$F = \begin{bmatrix} f_{11} & 0 \\ f_{21} & 0 \end{bmatrix} \quad (11)$$

### C. Reduced-order estimator

A reduced-order estimator is used to estimate the value of the body slip angle. Equations (12) and (13) yield the value of the estimated body slip angle  $\hat{\beta}$ .

$$\dot{\hat{\beta}}_c = \left( \frac{C_r}{mV} - L \frac{-bC_r}{J} \right) \hat{\beta} + \left( \frac{-bC_r}{mV^2} - 1 - L \frac{b^2C_r}{VJ} \right) r + \left[ \left( \frac{s}{tmV} \quad 0 \right) - L \left( \frac{c}{2} + \frac{as}{tJ} \quad \frac{c}{2} \right) \right] \begin{bmatrix} \Delta F_{lf} \\ \Delta F_{lr} \end{bmatrix} \quad (12)$$

$$\hat{\beta} = \hat{\beta}_c + Lr \quad (13)$$

### D. Individual tire forces computation

Least square estimation is used to compute the individual tire forces that will serve as the reference to the individual wheel brake controllers. Equation (14) gives the values of each individual wheel force as a function of the differential longitudinal force at front tires.

$$\begin{bmatrix} F_{lfl} \\ F_{lfr} \\ F_{lrl} \\ F_{lrr} \end{bmatrix} = \frac{1}{2} \begin{bmatrix} \Delta F_{lf} \\ -\Delta F_{lf} \\ \Delta F_{lr} \\ -\Delta F_{lr} \end{bmatrix} \quad (14)$$

## V. SIMULATION RESULTS

The simulations were carried out for different values of the commanded steering wheel angle  $\delta_w$ , for different values of the center of gravity speed  $V$ , and for different values of the scrub radius  $s$ . The results of the closed-loop control simulations were compared with experimentally verified simulation data from a car with a conventional steering system, which were provided by Ford Motor Company. The numerical values of the geometric parameters used in the simulation model corresponding to the provided data are shown in Table I. Although defined as positive in Figure 1, the values of the scrub radius used in the simulations are negative because most commercial cars have negative scrub radius.

TABLE I

VEHICLE PARAMETERS USED IN THE DEVELOPMENT OF THE SIMULATION MODEL.

Parameter	Value
$a$	1.046 m
$b$	1.712 m
$c$	1.55 m
$C_f$	-1090 N/deg
$C_r$	-1090 N/deg
$J$	3007 Kg $m^2$
$m$	1741.6 Kg
$s$	-0.02 m, -0.01 m, -0.005 m, -0.001 m
$t$	0.025 m
$SR$	17

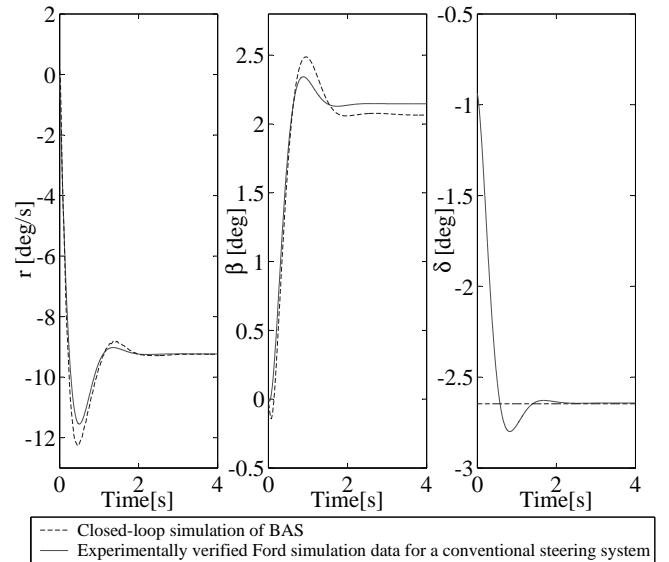


Fig. 4. Body slip angle  $\beta$ , yaw rate  $r$  and road wheel angle  $\delta$ , versus time for a  $-45^\circ$  step in steering wheel angle  $\delta_w$ , and 100 km/h vehicle speed  $V$ .

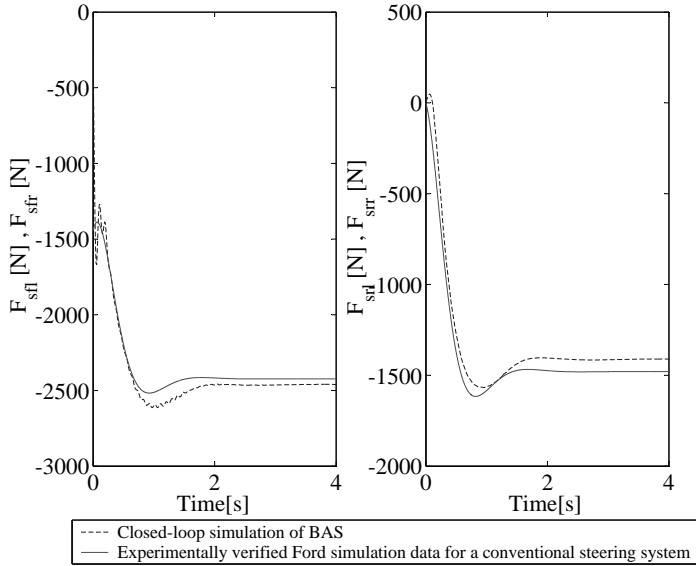


Fig. 5. Lateral forces acting on front and rear tires  $F_{sfl}$ ,  $F_{sfr}$ ,  $F_{srl}$ ,  $F_{srr}$ , versus time for a  $-45^\circ$  step in steering wheel angle  $\delta_w$ , and 100 km/h vehicle speed  $V$ .

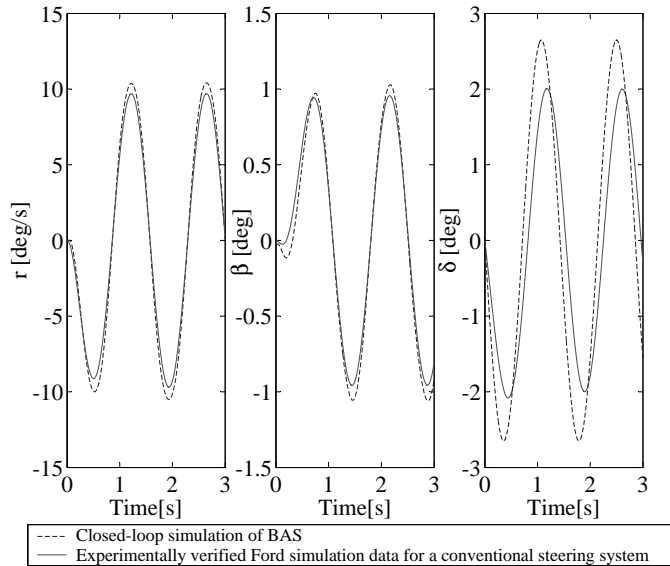


Fig. 6. Body slip angle  $\beta$ , yaw rate  $r$  and road wheel angle  $\delta$ , versus time for a  $45^\circ$ , 0.7 Hz sinusoidal steering wheel angle input  $\delta_w$ , and 70 km/h vehicle speed  $V$ .

Figures 4 and 5 show the results for one of the simulations carried out, corresponding to a step in steering wheel angle of  $-45^\circ$ , and a vehicle speed of  $V=100$  km/h. The dashed lines correspond to the experimentally verified behavior of the vehicle with a conventional steering system, while the solid lines show the simulation results of a model of the same vehicle implementing the BAS system. In Figure 4 the body slip angle  $\beta$ , the yaw rate  $r$  and the road wheel angle  $\delta$  are represented versus time. It can be seen that the shape of the yaw rate of a car with a conventional steering system

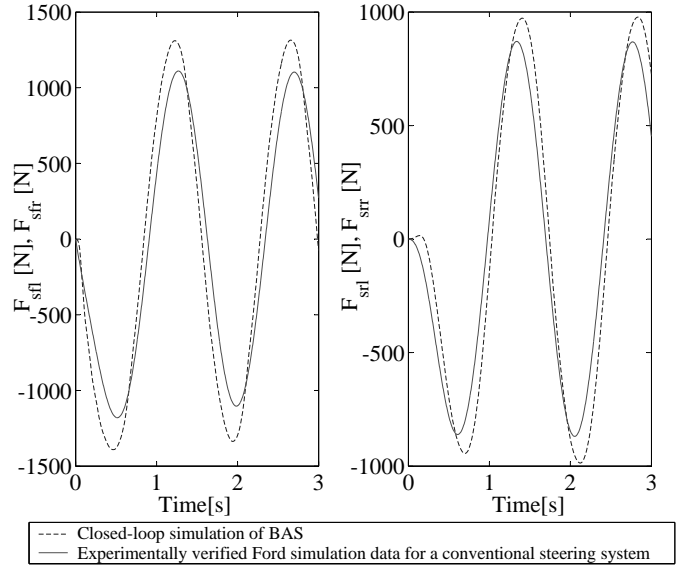


Fig. 7. Lateral forces acting on front and rear tires  $F_{sfl}$ ,  $F_{sfr}$ ,  $F_{srl}$ ,  $F_{srr}$ , versus time for a  $45^\circ$ , 0.7 Hz sinusoidal steering wheel angle input  $\delta_w$ , and 70 km/h vehicle speed  $V$ .

is matched almost perfectly, while the matching of the body slip angle is not perfect. The simulation results for the body slip angle have less overshoot than the verified data, while the steady-state value is bigger. These results are expected since the model reference used in the closed-loop simulations is a very simplified model of the dynamics of a car. Figure 5 displays the lateral forces acting on the tires  $F_{sfl}$ ,  $F_{sfr}$ ,  $F_{srl}$ ,  $F_{srr}$ , while cornering. Again, the matching between the experimentally verified data and the simulations is not perfect. In this case, the experimentally verified data displayed for  $F_{sfl}$ ,  $F_{sfr}$ ,  $F_{srl}$ ,  $F_{srr}$  corresponds to the average of the lateral forces acting on the tires of the same axle. In a real car, although having similar values, the lateral forces developed by the tires of the same axle are not exactly the same. Figures 6 and 7 show the results corresponding to a  $45^\circ$ , 0.7 Hz sinusoidal steering wheel angle input  $\delta_w$ , and 70 km/h vehicle speed  $V$ . Again, the discrepancy between the experimentally verified data and the simulations is expected since the model reference is a simplified vehicle dynamics model.

TABLE II  
STEADY-STATE VALUES OF THE TOTAL FORCES ACTING ON THE TIRES  $F_{tfl}$ ,  $F_{tfr}$ ,  $F_{trl}$ ,  $F_{trr}$  FOR A  $-45^\circ$  STEP IN STEERING WHEEL ANGLE, 100 km/h VEHICLE SPEED  $V$ , AND DIFFERENT VALUES OF SCRUB RADIUS  $s$ .

$s$ [m]	-0.001	-0.005	-0.01	-0.02
$F_{tfl}$ [N]	60,570	12,344	6,519	3,877
$F_{tfr}$ [N]	60,570	12,344	6,519	3,877
$F_{trl}$ [N]	60,891	12,264	6,265	3,384
$F_{trr}$ [N]	60,891	12,264	6,265	3,384

Table II shows the results corresponding to the the steady-state values of the total forces acting on the tires  $F_{tfl}$ ,  $F_{tfr}$ ,  $F_{trl}$ ,  $F_{trr}$ , also for a step in steering wheel angle of  $-45^\circ$ , and a vehicle speed of  $V=100$  km/h. It is very important to note that as the absolute value of the scrub radius decreases, the value of the total forces increases almost linearly. This result is very important and has to be handled carefully in the implementation of BAS since the adhesion limit of the tires is very important for the feasibility of the system.

## VI. CONCLUSIONS AND FUTURE WORK

This analysis indicates that within a reasonable envelope of scrub radius and braking force, Brake-Actuated Steering can be used to steer a vehicle with dynamic behavior similar to that of a car with a conventional steering system. Implementation of the proposed system, as well as SbW, will rely heavily on power electronics, electrical actuators, sensors and sophisticated control systems, some of which are already available in electronic stability systems.

The simulation results obtained in this paper were obtained with a simplified vehicle model. The next step would be to develop and evaluate a more accurate model including features such as a more accurate steering geometry, steering system compliance, load transfer, a road model including friction coefficients and a non-linear tire model. The implementation issues of the system are another important piece of future work that needs to be addressed.

## ACKNOWLEDGMENT

The authors would like to acknowledge Joseph Neal at Ford Motor Company for providing the vehicle dynamics data. Thanks are also extended to Robert Hammett at the Charles Stark Draper Laboratory and Douglas Milliken at Milliken Research Associates for helpful discussions and comments. This research was supported by the MIT/Industry Consortium on Advanced Automotive Electrical/Electronic Components and Systems.

## NOTATION

$a$ : Distance  $CG$  to front axle  
 $b$ : Distance  $CG$  to rear axle  
 $c$ : Distance between wheels on front and rear axles  
 $CG$ : Vehicle center of gravity  
 $C_f$ : Front axle equivalent cornering stiffness  
 $C_r$ : Rear axle equivalent cornering stiffness  
 $F$ : State feedback matrix  
 $F_{lfl}$ : Longitudinal force acting on the front left tire  
 $F_{lfr}$ : Longitudinal force acting on the front right tire  
 $F_{trl}$ : Longitudinal force acting on the rear left tire  
 $F_{trr}$ : Longitudinal force acting on the rear right tire  
 $F_{sfl}$ : Lateral force acting on the front left tire  
 $F_{sfr}$ : Lateral force acting on the front right tire  
 $F_{srl}$ : Lateral force acting on the rear left tire  
 $F_{srr}$ : Lateral force acting on the rear right tire  
 $F_{tfl}$ : Total force acting on the front left tire

$F_{tfr}$ : Total force acting on the front right tire  
 $F_{trl}$ : Total force acting on the rear left tire  
 $F_{trr}$ : Total force acting on the rear right tire  
 $J$ : Yaw inertia  
 $L$ : Observer gain  
 $m$ : Mass  
 $N_u$ : Zero steady-state error matrix gain  
 $r$ : Yaw rate  
 $r_r$ : Yaw rate reference  
 $s$ : Scrub radius  
 $SR$ : Total steering ratio  
 $t$ : Mechanical trail  
 $V$ :  $CG$  speed  
 $V_{fl}$ : Front left wheel center speed  
 $V_{fr}$ : Front right wheel center speed  
 $V_{rl}$ : Rear left wheel center speed  
 $V_{rr}$ : Rear right wheel center speed  
 $\Delta F_{lf}$ : Differential longitudinal force at the front tires  
 $\Delta F_{lr}$ : Differential longitudinal force at the rear tires  
 $\alpha_{fl}$ : Front left wheel slip angle  
 $\alpha_{fr}$ : Front right wheel slip angle  
 $\alpha_{rl}$ : Rear left wheel slip angle  
 $\alpha_{rr}$ : Rear right wheel slip angle  
 $\beta$ : Body slip angle  
 $\beta_c$ : Reduced-order observer state variable  
 $\beta_r$ : Body slip angle reference  
 $\hat{\beta}$ : Estimated body slip angle  
 $\delta$ : Road wheel angle  
 $\delta_w$ : Steering wheel angle

## REFERENCES

- [1] W. Harter, W. Pfeiffer, P. Dominke, G. Ruck, and P. Blessing, "Future electrical steering systems: Realizations with safety requirements," *SAE Technical Paper Series, Paper 2000-01-0822*, 2000.
- [2] P. Dominke and G. Ruck, "Electric power steering, the first step on the way to steer-by-wire," *SAE Technical Paper Series, Paper 1999-01-0401*, 1999.
- [3] R. Isermann, R. Schwarz, and S. Stolzl, "Fault-tolerant drive-by-wire systems," *IEEE Control Systems Magazine*, vol. 22, no. 5, 2002.
- [4] R. C. Hammett and P. S. Babcock, "Achieving  $10^{-9}$  dependability with drive-by-wire systems," *SAE Technical Paper Series, Paper 2003-01-1290*, 2003.
- [5] T. Tucker, "Touchdown: the development of propulsion controlled aircrafts at nasa dreyden," Monograph in aerospace history, no. 16, NASA, 1999.
- [6] BOSCH, *Driving-Safety Systems*. Robert Bosch GmbH, 2<sup>nd</sup> ed., 1999.
- [7] J. Guldner, M. Krug, S. Bakaus, K. Balszuweit, H. Smakman, C. Ebner, M. Graf, A. Schedl, P. Mescher, R. Disser, J. Heinrichs, S. Millsap, B. Murray, D. Krukenkamp, and M. Byers, "Back-drivable steer-by-wire system with positive scrub radius." US Patent Application Publication, December 2003.
- [8] W. Milliken and D. Milliken, *Race car vehicle dynamics*. Society of Automotive Engineers, 1995.
- [9] G. Franklin, J. D. Powell, and A. Emami-Naeini, *Feedback Control of Dynamic Systems*. Addison-Wesley, 1994.